Chitosan from Shrimp Waste/ Pd Nanoparticles/Ionic Liquids in Hydrogenation Reaction: Focus on Sustainability

Daiane K. Fischer
Laboratory of Catalysis and Nanomaterials, School of Chemistry and Food, Universidade Federal do Rio Grande – FURG

Karina Fraga
Laboratory of Catalysis and Nanomaterials, School of Chemistry and Food, Universidade Federal do Rio Grande – FURG

Carla W. Scheeren
Laboratory of Catalysis and Nanomaterials, School of Chemistry and Food, Universidade Federal do Rio Grande – FURG

ABSTRACT: Palladium nanoparticles (*ca. 4.8* nm) were supported in Chitosan microspheres/Ionic Liquids using a biopolymer solution of chitosan in acetic acid. The Pd NPs were synthesized in ILs 1-*n*-butyl-3-methylimidazolium bis(trifluoromethylsulfonyl) imide and 1-*n*-butyl-3-methylimidazolium hexafluorophosphate. The obtained material (Pd NPs/Chitosan/ ILs) was characterized and analyzed by the techniques of XRD, TEM, SEM and EDX, FAAS, IR and BET, to evaluate the texture of the material as well as the composition, homogeneity, structure and surface area. The presence of ILs exhibited greater stability and durability to the formed material (Pd NPs/IL/ Chitosan). The catalyst exhibited high catalytic activity when compared to Pd NPs only; this fact is related possibly to the large surface area and the durability provided by the support of the biopolymer.

INTRODUCTION

Solid supports with Pd catalysts were used in various industrial processes including hydrogenation 'Suzuki–Miyaura' coupling, naphtha reforming, oxidation, automotive exhaust catalysts and fuel cells.[1–8]

Chitosan is a natural biopolymer usually applied as a support to stabilize nanoparticles (NPs) and to prevent nanoparticle agglomeration.[9] The chemical interaction between the biopolymer and the metallic nanoparticles improves the durability and adhesion. The chitosan can be dissolved in dilute weak acid solutions due to the protonation of its amino groups, with acetic acid being the most commonly used solvent. The high presence of hydroxyl groups and amino groups in the polymer chain increases the hydrophilicity of chitosan, allowing its use as biomaterial. This biopolymer can be physically modified, one of the most interesting advantages being its great versatility in being prepared in different forms, such as powders, films, gels, hydrogels, flakes, microspheres, nanoparticles, membranes, sponges, fibers and nanofibers.[10–12]

The development of heterogeneous palladium catalysts proved to be promising for several reasons, including simple handling, easy recovery and efficient recycling. Therefore, the development of highly active, eco-friendly and recyclable heterogeneous palladium catalysts has become an important issue for the research into nanomaterials.[13–15] Recent attempts to develop highly efficient and recyclable Pd catalysts for the Heck, Suzuki and Sonogashira coupling and hydrogenation reactions have been focused mainly on the utilization of supports such as alumina, carbon, silica and biopolymers.[16–19]

Ionic liquids (ILs) in combination with solid supports have shown good results in the stability of metal nanoparticles.[20,21] Due to ILs being present pre-organized structures, these can induce structural directionality.[22–24] The ILs can adapt to other molecules due to their strong hydrogen bonding interactions; in this way, these compounds become attractive for the synthesis of nanostructured materials. [25–28]

Metal nanoparticles can be prepared by different methods, such as H_2 reduction of metal compounds or by simple decomposition of organometallic species dissolved in ILs. These nanoparticle synthesis methods can also combine other stabilizing species to form more stable and active nanomaterials.[29-33]

We present herein our results, which show that Pd NPs synthesized in the ILs [BMI.N(Tf)$_2$] and [BMI.PF$_6$] and supported in combination with chitosan solutions in acetic acid for the generation of heterogeneous catalysts, Pd NPs/IL/Chitosan. The catalytic activity was evaluated in hydrogenation reactions.

EXPERIMENTAL SECTION

General

All experiments were performed in air, except for the synthesis of the Pd NPs. The Pd NPs[34] and the halide-free functionalized ILs [BMI.PF$_6$] and [BMI.N(Tf)$_2$][35] were prepared according to literature procedure. Solvents, alkenes and arenes were dried with the appropriate drying agents and distilled under argon prior to use. All other chemicals were purchased from commercial sources and used without further purification. Gas chromatography analysis was performed with a Hewlett-Packard 5890 gas chromatograph with an FID detector and a 30 m capillary column with a dimethylpolysiloxane stationary phase. The NP formation and hydrogenation reactions were carried out in a modified Fischer–Porter bottle immersed in a silicone oil bath and connected to a hydrogen tank. The temperature was maintained at 75 °C by a stirring hot-stirring plate.

Synthesis of Pd NPs supported in chitosan microspheres

Chitosan was obtained from shrimp waste (Penaeus brasiliensis) according to the procedure described in the literature.[36] Deacetylation of chitin was carried out with sodium hydroxide solution (421 g L^{-1}) at 130 ± 1 °C, under constant agitation and reaction time of 4 h. Chitosan was purified by dissolution in acetic acid solution (1%). The solution was centrifuged for the removal of insoluble material. Total precipitation of chitosan was achieved by addition of sodium hydroxide solution to pH 12.0, followed by neutralization to pH 7.0. The chitosan suspension was centrifuged for separation of the supernatant and the chitosan paste dried in a spouted bed. Degree of deacetylation was determined by potentiometric linear titration, (chitosan from shrimp shells ≥81% deacetylated with molar mass 7.82×10^4 g mol^{-1}), and the chitosan molecular weight was measured by a viscosimetric method using the Mark–Houwink–Sakurada equation (K = 1.8×10^{-3} mL g^{-1} and α = 0.93).

Palladium acetylacetonate [Pd(acac)$_2$] (ACS reagent ≥99.0%), acetic acid (CH$_3$COOH) (ACS reagent ≥99.7%) and ammonium hydroxide (NH$_4$OH) (P.A reagent ≥98%) were purchased from Sigma-Aldrich, Brazil. All solutions were prepared with deionized water (18 MΩ cm, Milli-Q Millipore). Chitosan (Ch) solution (100 mL, 1.8% m/v in acetic acid 2%) was prepared under agitation for 24 h. Subsequently, a solution containing 10 mg of Pd NPs dispersed in 1.0 g of ILs [BMI.PF$_6$] or [BMI.N(Tf)$_2$] was added. The solution obtained (containing chitosan solution and Pd NPs in ILs) was added dropwise into 200 mL ammonium hydroxide (NH$_4$OH) solution (50% v/v) via a syringe equipped with a 21 mm needle of 0.8 mm diameter. The spheres formed were washed with distilled water and dried at 40 °C.

X-ray diffraction (XRD)

The phase structures of Pd NPs synthesized in ILs were characterized by XRD. For XRD analysis, the NPs were isolated as fine powder and placed on the specimen holder. The XRD experiments were performed in a SIEMENS D500 diffractometer equipped with a curved graphite crystal using Cu Ka radiation (l = 1.5406 Å). The diffraction data were collected at room temperature in Bragg-Brentano geometry q–2q. The equipment was operated at 40 kV and 20 mA with a scan range between 20° and 90°. The diffractograms were obtained with a constant step D 2q = 0.05. The indexation of Bragg reflections was obtained by fitting a pseudo-Voigt profile using the FULPROFF code.[37]

Infrared analysis of Chitosan and Pd NPs/ILs/Chitosan

The infrared spectra of the pure chitosan microspheres and Pd NPs/ILs/Chitosan were obtained using a Shimadzu FTIR, model 8300. The spectra were obtained at room temperature with a resolution of 4 cm^{-1} and 100 cumulative scans.

Nitrogen adsorption–desorption isotherms

The adsorption–desorption isotherms of previously degassed solids (150 °C) were determined at liquid nitrogen boiling point in a volumetric apparatus, using nitrogen as probe. The specific surface areas of the materials were determined from the *t*-plot analysis, and pore size distribution was obtained using the BJH method. Specially designed equipment with a vacuum line system employing a turbo-molecular Edwards vacuum pump was used. The pressure measurements were made using a capillary Hg barometer and a Pirani gauge.

Scanning Electron Microscopy (SEM) and Electron Dispersive Spectroscopy (EDS) elemental analysis

The Pd NPs/IL/Chitosan materials were analyzed by SEM using a JEOL model JSM 5800 with 20 kV and 5000× magnification. The same instrument was used for the EDS analysis with a Noran detector (20 kV and acquisition time of 100 s and 5000× magnification).

Transmission Electron Microscopy (TEM) analysis

The morphologies and the electron diffraction (ED) patterns of the biopolymeric materials were determined on a JEOL JEM-2010 equipped with an EDS system and a JEOL JEM-120 EXII electron microscope, operating at accelerating voltages of 200 and 120 kV, respectively. The TEM samples were prepared by deposition of the Pd NPs

or Pd NPs/ILs/Chitosan on a carbon-coated copper grid at room temperature. The histograms of the Pd NP size distributions were obtained from the measurement of around 300 diameters and reproduced in different regions of the Cu grid, assuming spherical shapes.

Catalytic hydrogenations

The catalyst Pd NPs/ILs/Chitosan (150 mg) was placed in a Fischer–Porter bottle and the alkene or arene (12.5 mmol) was added. The reactor was placed in an oil bath at 75 °C and hydrogen was admitted to the system at constant pressure (4 atm) under stirring until the consumption of hydrogen stopped. The organic products were recovered by decantation and analyzed by GC. The re-use of the catalysts was performed by simple extraction of the organic phase (upper phase) followed by the addition of the arene or alkene.

RESULTS AND DISCUSSION

Chitosan is a modified biopolymer, derived by partial deacetylation of chitin. This compound may exhibit different degrees of deacetylation, but when the degree of deacetylation of chitin reaches about 50%, it becomes soluble in aqueous acidic media and is called chitosan.[9,10] The solubilization occurs due to protonation of the $-NH_2$ function at the C-2 position of the d-glucosamine repeat unit. As the compound shows good solubility in aqueous solutions, it is used widely in different applications, such as fibers, films, membranes, gels, solutions or spheres.[11–13] The addition of sodium hydroxide or ammonium hydroxide causes flocculation due to deprotonation and insolubility of the polymer. The polymer is then washed with water and dried.

Chitosan microspheres containing supported Pd NPs were prepared using the combination of biopolymeric solution of chitosan in acetic acid and palladium acetylacetonate $[Pd(acac)_2]$ in $[BMI.PF_6]$ and $[BMI.N(Tf)_2]$ ILs. The Pd NP synthesis was performed by hydrogen reduction (4 atm) of $[Pd(acac)_2]$ dispersed in the $[BMI.PF_6]$ and $[BMI.N(Tf)_2]$ ILs at 75 °C.[34]

The XRD analysis clearly identified crystalline palladium in the isolated material. The diffraction lines (111, 200, 220, 311, 222) of metallic Pd can be observed in the diffraction pattern (Figure 1). The Pd NPs obtained presented sizes of 4.8 ± 0.4 nm with a narrow diameter distribution range.
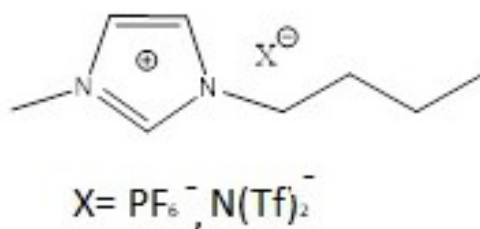
**Scheme 1.** Structure of the ILs applied in this work.
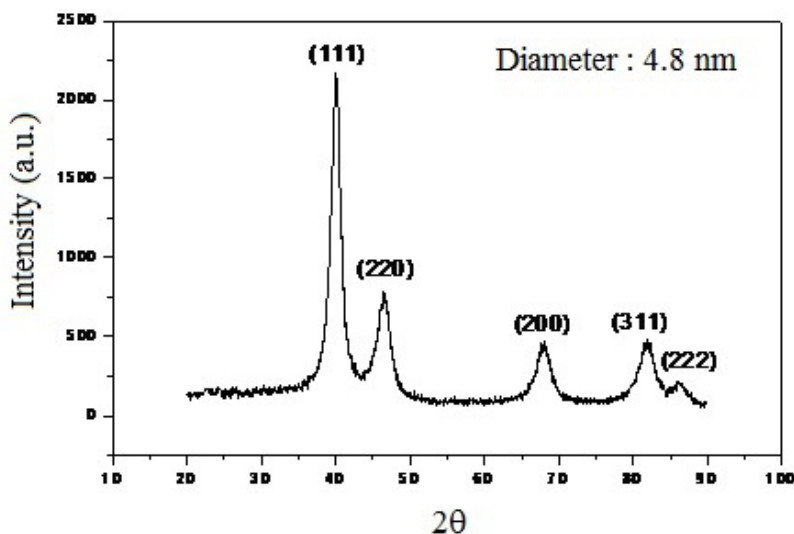
Figure 1. XRD analysis of Pd NPs (4.8 nm) synthesized in ionic liquid [BMI.PF$_6$].

Figure 2 shows the FT-IR spectra of pure chitosan microspheres (Figure 2A) and Pd NPs/ILs/Chitosan (Figure 2B). In Figure 2A, it is possible to observe the characteristic bands of the chitosan. The bands in the range 3400–3200 cm^{-1} are related to N–H and O–H stretching. Stretching vibrations of amide C=O are seen at 1658 cm^{-1}. Angular vibrations of N–H are observed at 1550 cm^{-1}, and the N–C stretching vibrations are identified at 1156 cm^{-1}. The band at 1414 cm^{-1} can be attributed to the CH$_2$ stretching. The band in 1018 cm^{-1} can be assigned to the C–O stretching.

In Figure 2B, the Pd NPs/ILs/Chitosan spectrum shows the N–H and O–H stretching bands at 3312 cm^{-1}, and at 1633 cm^{-1} the stretching vibrations of C=O, where

both showed a decrease, possibly due to the presence of ionic liquid and Pd NPs. After addition of the IL to the chitosan, a significant decrease was observed in the intensity of the band at 3312 cm^{-1}, attributed to the –OH stretching of the pure chitosan microspheres, indicating participation of the –OH group in the interaction with the positive surfaces of the IL and the Pd NPs. At 1560 cm^{-1} a decrease in the N–H band relative to the angular vibrations was observed. This change is possibly related to the interaction of the positive charge density of the Pd NPs with the free nitrogen lone pair (NH$_2$).

The CH$_2$ band at 1414 cm^{-1} relative to bending vibrations in Figure 2A was not pronounced in the Pd NPs/ILs/Chitosan spectrum (Figure 2B). The band at 1156 cm^{-1} attributed to the N–C stretching, and the band in 1018 cm^{-1} assigned to the C–O stretching, both decreased. This can be due to the presence of Pd NPs in the chitosan, which led to a stabilization of the biopolymer functional groups, hindering the conversion of radiation into vibrational energy
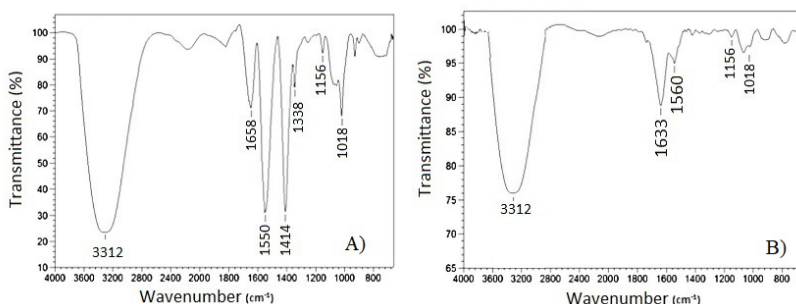
**Figure 2.** Infrared spectra of the pure chitosan microspheres and Pd NPs/ILs/Chitosan.

The metal distribution in the support was determined by SEM-EDX analysis. The mapping showed a homogeneous Pd NPs distribution over the surface of the chitosan microspheres (Figure 3). The micrograph shows lighter regions, indicating the presence of palladium metal NPs on the chitosan microspheres (gray regions). The elemental composition of the region focused on the micrograph confirms this structure.
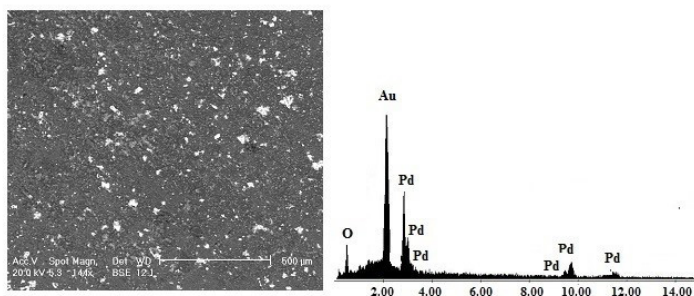
Figure 3. SEM micrographs illustrating the heterogeneous distribution
of Pd NPs in biopolymeric surface of the chitosan microspheres
(Pd NPs/IL/ BMI.N(Tf)$_2$) and corresponding EDX.

Sample Pd NPs/IL/Chitosan was analyzed by the scanning point and area exposed to the electron beam. All selected areas showed the presence of Pd in the chitosan microspheres. In the micrograph, the metal is identified by the bright regions in contrast to the array of chitosan biopolymer that has the dark background.

Figures 4 illustrates the micrographs of Pd NPs/IL/Chitosan microspheres obtained by SEM. In the case of Pd NPs/BMI.N(Tf)$_2$ IL/Chitosan, spherical particles were observed (Figure 4).
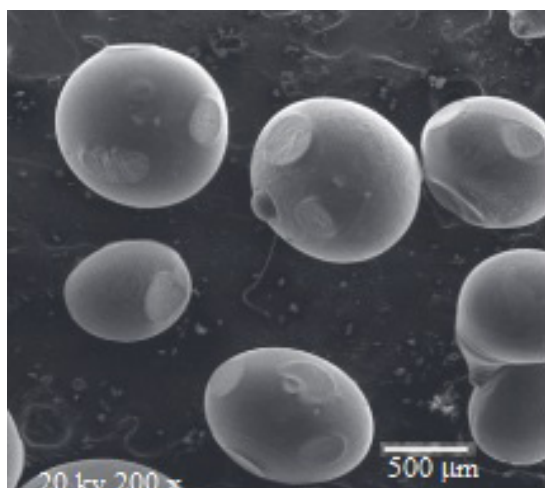
Figure 3. Micrographs obtained by SEM of the resulting Chitosan
microspheres containing Pd [Pd NPs/[BMI.N(Tf)$_2$]IL/Chitosan].

TEM was employed for the characterization of the supported catalyst. Figure 5 (top) shows the micrograph of the isolated Pd NPs [BMI.PF$_6$], and their mean size, which was shown to be *ca.* 4.8 nm. In the case of Pd NPs BMI.PF$_6$/Chitosan, Figure 5, both the morphology and size (*ca.* 4.8 nm) were maintained within the chitosan microspheres. It is very likely that the presence of ionic liquid affords stability, avoiding sintering of the metallic particles.
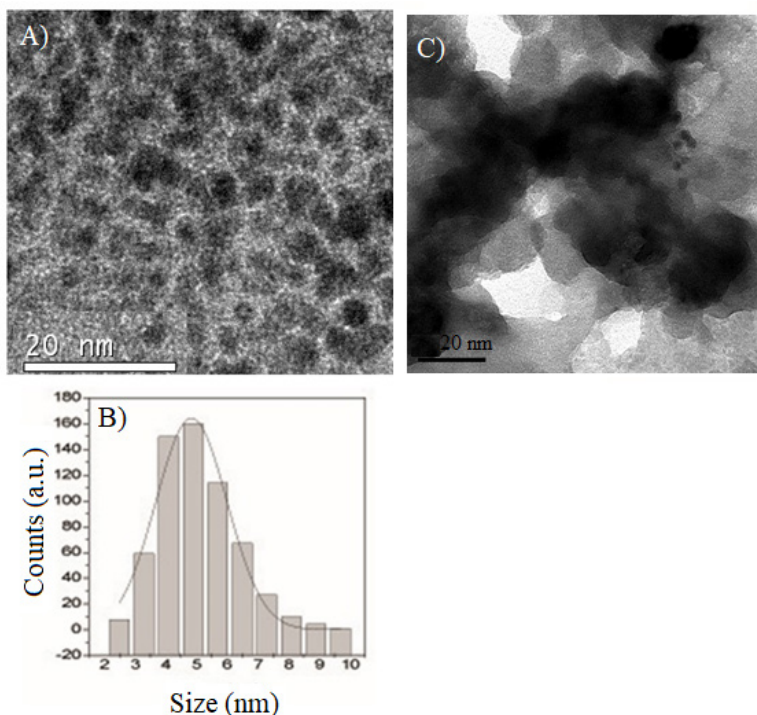
Figure 5. TEM micrographs of: A) Pd NPs in the BMI.N(Tf)$_2$ ionic liquid, B) Histogram showing the particle size of Pd NPs in the BMI.N(Tf)$_2$ ionic liquid and C) Chitosan microspheres containing Pd NPs.

The textural properties were further characterized by nitrogen adsorption. The specific area was calculated by the BET method, while pore diameter, by BJH (Table 1). According to Table 1, the pure chitosan microspheres prepared in the absence of Pd/ILs presented higher specific area (*ca.* 200 m^2 g^{-1}). The introduction of Pd NPs/ILs during the synthesis led to a reduction in the specific area. The supported catalysts were evaluated in hydrogenation reactions.

Entry	Sample	SBET/m² g⁻¹	Vp/cm³ g⁻¹	dp/nm
1	Pure Chitosan nanospheres	220	0.6	9.4
3	Pd NPs [BMI.PF$_6$]/Chitosan	151	0.2	2.3
4	Pd NPs [BMI.N(Tf)$_2$]/ Chitosan	186	0.5	4.6

[a]S_{BET} = specific area determined by BET method. *Vp* = pore volume, *dp* = pore diameter.

Table 1. Surface area, pore volume and average pore diameter of Pd NPs/IL/Chitosan[a].

Table 2 presents data regarding 1-decene, cyclohexene and benzene hydrogenation reactions. For comparative purposes, we also include the data concerning the catalytic activity of isolated Pd NPs. In the benzene hydrogenation experiments, the product obtained was always cyclohexane.

Table 2 shows the results obtained in the hydrogenation reactions using the system Pd NPs/IL/Chitosan. For comparison, effects were added results using only the Pd NPs in hydrogenation reactions (Entries 8–10, Table 2). Is possible to observe that the supported systems were more active than those constituted of only Pd NPs.

| Entry	Catalyst	Ionic Liquid	Substrate	Time (h)	TOF (h⁻¹)	TOF (h⁻¹)[c]
1	Pd NPs/ IL/Chitosan	BMI.N(Tf)$_2$	1-Decene	0.15	416	1067
2	Pd NPs/ IL/Chitosan	BMI.PF$_6$	1-Decene	0.4	156	400
3	Pd NPs/ IL/Chitosan	BMI.N(Tf)$_2$	Cyclohexene	0.8	78	200
4	Pd NPs/ IL/Chitosan	BMI.PF$_6$	Cyclohexene	1.2	52	133
5	Pd NPs/ IL/Chitosan	BMI.N(Tf)$_2$	Benzene	1.8	35	90
6	Pd NPs/ IL/Chitosan	BMI.PF$_6$	Benzene	2.5	25	64
7	Pd NPs/ IL/Chitosan	BMI.PF$_6$	1-Decene	0.2	312	801
8	[b]Pd NPs	-	1-Decene	0.9	28	72
8	[b]Pd NPs	-	Cyclohexene	1.6	16	41
10	[b]Pd NPs	-	Benzene	10	2.5	6.4

[a]Conditions: H$_2$ pressure 4 atm, temperature 75 °C, ratio [alkene/arene]/[Pd/IL/ Chitosan] = 625:1, added Pd NPs/IL/Chitosan 150 mg, 0.025 mmol Pd, followed by 12.5 mmol of alkenes or arenes used. [b]Pd nanoparticles 10 mg, ratio [arene]/ [Pd] = 250:1, added Pd (10 mg), followed by 12.5 mmol of the alkenes or arenes used. Turnover frequency (TOF) values were calculated for 10% conversion. TOF[c] values corrected values for atoms exposed on the surface (39%).

Table 2. Hydrogenation of alkenes/arene by Pd NPs/ILs/Chitosan[a] and Pd NPs[b].

The catalytic activity of the heterogeneous catalysts prepared in this work were expressed using the turnover frequency (TOF), (the TOF values were estimated for low substrate conversions, 10%), and they were also corrected by the number of exposed surface atoms by using the metal atom's magic number approach.[38]

The more organized structure generated under $BMI.N(Tf)_2$ IL might have afforded more active systems, as shown by the observed hydrogenation results. The ionic liquid content, which seems to be important in order to guarantee stability for the NPs, was higher for these systems. Besides, according to porosimetric measurements, the pore diameter was much higher for the Pd $NPs/BMI.N(Tf)_2$ IL/Chitosan. The hydrogenation of simple arenes and alkenes by Pd NPs/IL/Chitosan depends on steric hindrance at the C=C double bond and follows the same trend as observed with classical palladium complexes in homogeneous conditions; that is, the reactivity follows the order: terminal–internal. The supported catalytic material can be recovered by simple decantation and re-applied at least four times without any significant loss in catalytic activity. The biopolymeric supported catalyst maintains its activity after four recycles, demonstrating some loss of catalytic activity in the last two recycles.
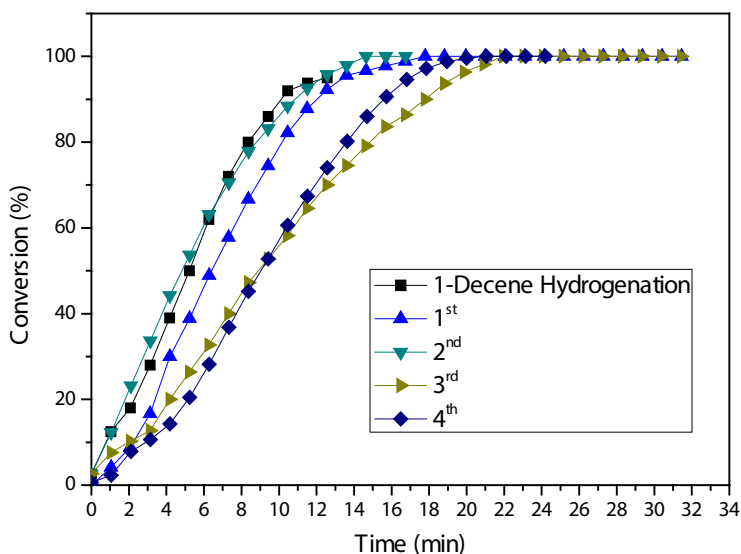
Figure 6. Conversion curves of 1-Decene hydrogenation by Pd NPs/BMI.N(Tf)$_2$ IL/Chitosan at 4 atm H$_2$ and 75 °C.

CONCLUSIONS

The Pd NPs synthesized from [Pd(acac)$_2$] in [BMI.PF$_6$] and [BMI.N(Tf)$_2$] ILs can be easily supported on chitosan microspheres. XRD analysis confirmed the presence of metallic palladium, TEM showed Pd NPs to be in a narrow diameter distribution range, with an average diameter of 4.8 nm. The BET analyses showed large surface area and pore diameter of the microspheres, a factor that proved to be fundamental to the catalytic activity obtained.

Based on the hydrogenation results it was possible to observe that the Pd NPs in ILs supported on chitosan microspheres were more active than when only palladium nanoparticles were used. This fact is related to the greater stability and durability of the supported materials in combination with the ILs. This combination exhibits an excellent synergistic effect, which increases the stability and the activity of the Pd in hydrogenation catalysis.

ACKNOWLEDGMENTS

REFERENCES

[a]Laboratory of Catalysis, and Nanomaterials, School of Chemistry and Food, Universidade Federal do Rio Grande – FURG, Rua Barão do Caí, 125, CEP 95500–000, Santo Antônio da Patrulha, RS, Brazil.*e-mail: carlascheeren@gmail.com

Ranjith, Kugalur Shanmugam; Celebioglu, Asli; Uyar, Tamer. Immobilized Pd-Ag bimetallic nanoparticles on polymeric nanofibers as an effective catalyst: effective loading of Ag with bimetallic functionality through Pd nucleated nanofibers. *Nanotechnology*, 29, 2018.

Vedyagin, A. A.; Plyusnim, P. E.; Rybinskaya, A. A.; Shubin, Y. V.; Mishakov, I. V.; Korenev, S. V. Synthesis and study of Pd-Rh alloy nanoparticles and alumina-supported low-content Pd-Rh catalysts for CO oxidation. *Materials Research Bulletin*. **102**, 2018, 196-202.

Guo, Z.; Liu, Y.; Liu, Y. Chu, W. Promising SiC support for Pd catalyst in selective hydrogenation of acetylene to ethylene. Applied Surface Science, **442** (2018) 736–74.

Wilson, M.; Kore,R.; Ritchie, A. W.; Fraser, R. C.; Beaumont, S. K.; Srivastava, R.; Baydal, J. P. S. Palladium–poly(ionic liquid) membranes for permselective sonochemical flow catalysis. *Colloids and Surfaces A: Physicochemical and Engineering Aspects*, **545**, 2018, 78-85.

Baran, T.; Baran, N. Y.; Mentes, A. Preparation, structural characterization, and catalytic performance of Pd(II) and Pt(II) complexes derived from cellulose Schiff base. *Journal of Molecular Structure*, **1160**, 2018, 154-160.

H. Hosseini, M. Mahyari, A. Bagheri, et al. Pd and PdCo alloy nanoparticles supported on polypropylenimine dendrimer-grafted graphene: A highly efficient anodic catalyst for direct formic acid fuel cells.Journal of Power Sources, 2014, **247**, 70.

Zhang, C.; Yu, H.; Li, Y.; Fu, L.; Gao, Y.; Song, W.; Shao, Z.; Yi, B. Highly stable ternary tin–palladium–platinum catalysts supported on hydrogenated TiO2 nanotube arrays for fuel cells. Nanoscale, 2013, 5, 6834–6841.

Kunfi, A.; May, Z.; Németh, P.; London, G.Polydopamine supported palladium nanoparticles: Highly efficient catalysts in Suzuki cross-coupling and tandem Suzuki cross-coupling nitroarene reductions under green reaction conditions. *Journal of Catalysis* 361 (2018) 84–93. https://doi.org/10.1016/j.jcat.2018.02.031

Manikandan, A.; Sathiyabama, M. Green Synthesis of Copper-Chitosan Nanoparticles and Study of its Antibacterial Activity. Journal of Nanomedicine & Nanotechnology. 2015, 6. DOI: 10.4172/2157-7439.1000251

Wang, D.; Lu, Q.; Wei, M.; Guo, E. Ultrasmall Ag nanocrystals supported on chitosan/PVA nanofiber mats with bifunctional properties. *Applied Polymer*. 135, 2018, 46504 (1-8). DOI: 10.1002/APP.46504

Habiba, U.; Siddique, T. A.; Lee, J. J. L.; Joo, T. C.; Ang, B. C.; Afifi, A. M. Adsorption study of methyl orange by chitosan/polyvinyl alcohol/zeolite electrospun composite nanofibrous membrane. *Carbohydrate Polymers*, 191 (2018) 79–85. https://doi.org/10.1016/j.carbpol.2018.02.08

Li, R.; Liu, Q.; Wu, H.; Wang, K.; Li, L.; Zhou, C.; Ao, N. Preparation and characterization of in-situ formable liposome/chitosan composite hydrogels. Materials Letters, 220, (2018), 289-292. https://doi.org/10.1016/J.matlet.2018.03.052

Lee, M.; Chen, B-Y.; Den, W. *Appl. Sci.* 2015, 5, 1272-1283.

Rinaudo, M. Chitin and chitosan: Properties and applications. *Prog. Polyme. Sci.* 31, 2006, 603-632.

Gore, P.M.; Khurana, L.; Siddique, S.; Panicker, A.; Kandasubramanian, B. Ion-imprinted electrospun nanofibers of chitosan/1-butyl-3-methylimidazolium tetrafluoroborate for the dynamic expulsion of thorium (IV) ions from mimicked effluents. *Environmental Science and Pollution Research International. 25, 2017, 3320-3334.* DOI: 10.1007/s11356-017-0618-6 .

He, M.; Chen, H.; Zhang, X.; Wang, C.; Xu, C.; Xue, Y.; Wang, J.; Zhou, P. Multifunctional Chitin Nanogels for Simultaneous Drug Delivery, Bioimaging, and Biosensing. *Cellulose,* 25, 2018, 1987-1996.

Shabbir, S.; Lee, S.; Lim, M.; Lee, H.; Ko, H.; Lee, Y.; Rhee, H. Pd nanoparticles on reverse phase silica gel as recyclable catalyst for Suzuki-Miyaura cross coupling reaction and hydrogenation in water. *Journal of Organometallic Chemistry*, 846, **296**, 2017.

Veerakumar, P.; Thanasekaran, P.; Lu, K. L.; Liu, S. B.; Rajagopal, S. Biomass Derived Sheet-like Carbon/Palladium Nanocomposite: An Excellent Opportunity for Reduction of Toxic Hexavalent Chromium. *ACS Sustainable Chemistry & Engineering*, 6357, **5**, 2017.

Ai, C. J.; Gong, G. B.; Zhao, X. T.; Liu, P. Macroporous hollow silica microspheres-supported palladium catalyst for selective hydrogenation of nitrile butadiene rubber. *Journal of the Taiwan Institute of Chemical Engineers*, 77, **250**, 2017.

Faria, V. W.; Oliveira, D. G. M.; Kurz, M. H. S.; Gonçalves, F. F.; Scheeren, C. W.; Rosa, G. R. Palladium nanoparticles supported in a polymeric membrane: an efficient phosphine-free "green" catalyst for Suzuki-Miyaura reactions in water. *RSC Advances*, 13446, **4**, ,2014.

Ulusal, F.; Darendeli, B.; Erunal, E.; Egitmen, A.; Guzel, B. Supercritical carbondioxide deposition of gamma-Alumina supported Pd nanocatalysts with new precursors and using on Suzuki-Miyaura coupling reactions. *Journal of supercritical fluids*, 127, **111**, 2017.

Hameed, R. M. A. Enhanced ethanol electro-oxidation reaction on carbon supported Pd-metal oxide electrocatalysts. *Journal of colloid and interface science*. 505, **230**, 2017.

Wen, Y.; Hsin-Wei, L.; Chung-Sung, T. Yu, W.; Lin, H-W.; Tan, C-S. Direct synthesis of Pd incorporated in mesoporous silica for solvent-free selective hydrogenation of chloronitrobenzenes. *Chemical Engineering Journal,* 325, 2017, 124-133.

(a) Mehnert, C. P. Supported ionic liquid phases . *Chem.–Eur. J.*, 2004, **11**, 50. (B) Gelesky, M. A.; Scheeren, C. W.; Foppa, L.; Pavan, F. A.; Dias, S. L. P.; Dupont, J. Metal Nanoparticle/Ionic Liquid/Cellulose: New Catalytically Active Membrane Materials for Hydrogenation Reactions. *Biomacromolecules*, 2009, **10**, 1888-1893.

Gelesky, M. A.; Chiaro, S. S. X.; Pavan, F. A.; Santos, J. H. Z.; Dupont, J. Supported ionic liquid phase rhodium nanoparticle hydrogenation catalysts.*Dalton Trans.*, 2007, **55**, 49.

A. Riisager, R. Fehrmann, M. Haumann and P. Wasserscheid. Supported ionic liquids: versatile reaction and separation media.*Top. Catal.*, 2006, **40**, 91.

J. Dupont and P. A. Z. Suarez. Physico-chemical processes in imidazolium ionic liquids. *Phys. Chem. Chem. Phys.*, 2006, **8**, 2441.

C. S. Consorti, P. A. Z. Suarez, R. F. de Souza, R. A. Burrow, D. H. Farrar, A. J. Lough,W. Loh, L. H. M. da Silva and J. Dupont. Identification of 1,3-dialkylimidazolium salt supramolecular aggregates in solution . *J. Phys. Chem. B*, 2005, **109**, 4341.

J. Dupont, *J.* On the solid, liquid and solution structural organization of imidazolium ionic liquids. *Braz. Chem. Soc.*, 2004, **15**, 341.

R, Linhardt, Q. M. Kainz,R. N. Grass, W. J. Stark,O. Reiser. Palladium nanoparticles supported on ionic liquid modified, magnetic nanobeads - recyclable, high-capacity catalysts for alkene hydrogenation. RSC Adv., 2014, **4**, 8541.

Y. Zhou. Recent advances in ionic liquids for synthesis of inorganic nanomaterials. *Cur. Nanosc.*, 2005, **1**, 35.

(a) C. W. Scheeren, G. Machado,J. Dupont,P. F. P. Fichtner,S. Texeira, *Inorg. Chem.* 2003, **42**, 4738. (b) C.W. Scheeren, G. Machado, S. R. Teixeira, J. Morais, J. B. Domingos and J. Dupont, *J. Phys. Chem. B*, 2006, **110**, 13011.(c) Dupont, J.; Fonseca, G. S.; Umpierre, A. P.; Fichtner, P. F. P.; Teixeira, S. R. Transition-metal nanoparticles in imidazolium ionic liquids: Recyclable catalysts for biphasic hydrogenation reactions. *J. Am. Chem. Soc.*, 2002, **124**, 4228. (d) Dupont, J.; Migowski, P. Catalytic applications of metal nanoparticles in imidazolium ionic liquids. *Chem.–Eur. J.,* 2007, **13**, 32.

X. D. Mu, D. G. Evans and Y. A. Kou. A general method for preparation of PVP-stabilized noble metal nanoparticles in room temperature ionic liquids. *Catal. Lett.*, 2004, **97**, 151.

Oliveira, D. G. M.; Rosa, G. R.; Scheeren, C. W. Rh and Pd Nanoparticles Supported in a Polymeric Membrane: Evaluation in Hydrogenation and Suzuki-Miyaura Reactions. *Journal of Nanoscience and Nanotechnology*, 2017, **17**, 1-7.

Cassol, C. C.;, Ebeling, G.; Ferrera, B.; Dupont, J. A simple and practical method for the preparation and purity determination of halide-free imidazolium ionic liquids. *Adv. Synth. Catal.*, 2006, **348**, 243.

Moura C. M, Moura J. M, Soares N. M, Pinto L. A. A. Kinetics and Mechanism of the Food Dye FD&C Red 40 Adsorption onto Chitosan. *Chem Eng Process Intensif.*, **50**, 2011, 351.

Carbajal, J. R. Short Reference Guide of The Program Fullprof version 3.5. Ftp://Charybde. Saclay.Cea.Fr

Umpierre, A. P.; Jesús, E.; Dupont, J. Turnover Numbers and Soluble Metal Nanoparticles. *ChemCatChem*, 2011, **3**, 1413.